THE EFFECT OF VARIOUS CUTTING ENVIRONMENTS ON TOOL WEAR AND ENERGY CONSUMPTION IN HIGH-FEED MILLING (HFM) OF TOOL STEEL

MARTIN DRBAL (0009-0002-4266-1598)[1], STEPAN KOLOMY (0000-0003-3781-692X)[1], ONDREJ VYSTRCIL (0009-0007-9558-2152)[1], JOSEF SEDLAK (0000-0002-9819-8259)[1], JAN ZOUHAR (0000-0001-8031-8366)[1], ALES JAROS (0000-0002-4405-409X)[1], JAN SEDLACEK (0009-0009-9431-7781)[1]

[1]Brno University of Technology, Faculty of Mechanical Engineering, Technicka 2 Brno, Czech Republic

DOI: 10.17973/MMSJ.2026_11_2026053

martin.drbal@vutbr.cz

High-Feed Milling (HFM) is a highly productive method for machining tool steels. However, selecting the optimal cutting environment remains a critical factor for ensuring tool life and energy efficiency. This study compares five different cooling strategies – dry machining, conventional external fluid cooling, high-pressure internal fluid cooling, cooling via compressed air through the spindle, and external compressed air nozzle cooling – during the milling of X37CrMoV5-1 (300 HB) tool steel. The evaluation focused on flank wear kinetics (VB_B), carbide tool degradation mechanisms, and total machine power consumption, followed by the determination of specific cutting energy and carbon footprint (CF_{1h}). The results demonstrated that liquid cooling leads to premature tool failure due to thermal shocks and comb cracking, reducing tool life by more than 50% compared to gaseous media. Energy analysis demonstrated that liquid cooling increases machine power consumption by approximately 1000 W and doubles the specific cutting energy compared to dry machining. The study confirmed that for this HFM application, compressed air cooling or dry machining is an optimal strategy from both a durability and machining sustainability perspective.

KEYWORDS

High feed milling (HFM), tool wear, carbon footprint, energy consumption, sustainable machining.

1 INTRODUCTION

High-feed milling (HFM) technology is a machining method characterized by high material removal rates. A combination of three key parameters is crucial for this technology: the axial depth of cut (a_p), the principal cutting edge angle (K_r), and the feed per tooth (f_z) [Jacquet 2025]. For HFM, the axial depth of cut and the principal cutting edge angle are always lower (ap is typically up to 2 mm, and Kr ranges between 10° and 20°) [Gylienė 2016]. This small principal cutting edge angle results in a longer contact area between the tool edge and the workpiece material. Due to this increased contact area, a low axial depth of cut ap must be selected. Otherwise, the cutting resistance and generated cutting forces would exceed the rigidity limits of both the tool and the machine tool [Bleicher 2018]. A higher feed per tooth f_z yields a higher feed rate v_f, which significantly influences the machining time and resulting surface integrity [Kuhlmann 2024]. In HFM technology, the ratio of the set feed to the tool radius is often between 0.2 and 0.4, whereas in conventional milling, this ratio typically ranges from 0.01 to 0.1 mm [Huang 2021]. For these reasons, HFM is faster compared to conventional milling, achieving a higher material removal rate (MRR) per unit of time, and generally provides users with a reduction in operating costs. Extreme feed rates in HFM technology alter the cutting physics and chip geometry. Under correct configurations, a chip thinning effect occurs, and the resultant cutting force acts primarily in the axial direction. The radial force component is almost negligible, which reduces vibrations and stabilizes the cutting process [Jacquet 2025]. This fact positively affects the tool life of cutting tools designated for this technology [Bleicher 2018]. Selecting higher values of feed per tooth f_z compensates for the low principal cutting edge angle and increases the width of the formed chip. Consequently, the cross-section of the chip leaving the cutting zone is characterized by a very thin and wide geometry [Jacquet 2025]. Given this modification in chip characteristics, a comparison between HFM and conventional milling methods is highly relevant. Studies demonstrate that a high material removal rate (MRR) can be achieved within a shorter timeframe due to the chip thinning effect and the specific distribution of cutting forces. This process efficiency leads to reduced machine loading and shorter machining times, which represents a key prerequisite for lowering the energy consumption of the machining process. Due to the specific kinematics of the process and rapid material evacuation in HFM, the vast majority of the generated heat is dissipated from the cutting zone directly via the chips, typically nearly 90% [Bleicher 2018]. This mechanism significantly reduces the thermal load on both the cutting tool itself and the surface layer of the workpiece. As a result, the chips from the HFM process exhibit intense temper colors. Shades of bronze, violet, and, in extreme cases, blue are typical. This coloration confirms a high concentration of heat transferred from the cutting process into the chip, with chip temperatures ranging between 220–350 °C, or even higher, during the cutting process, which can be evaluated precisely based on the coloration and structural deformation. One of the theoretical foundations is the fact that the application of cooling can be counterproductive during milling. Milling is generally considered an interrupted cutting process. Consequently, during the cutting operation, the tool edge is exposed to cyclic temperature increases followed by cooling periods (after the chip is detached). The temperature of the cutting edge thus fluctuates within a certain range throughout the machining time. If a cooling medium is introduced into this system, the thermal stress on the cutting edge becomes even more pronounced. The specific thermal dynamics of the HFM process are no exception, and the formation of this temperature gradient can act as a catalyst for the initiation of thermal cracks perpendicular to the cutting edge [Peters 1992]. Research in this field confirms that inappropriately selected tool geometry and processing conditions can lead to significant energy losses and accelerated tool wear, which ultimately increases overall manufacturing costs [Majerik 2015]. Mechanical wear of indexable inserts, manifesting as progressive flank wear, is often a consequence of a combination of excessive feed rates and local variations in the hardness of the workpiece material in HSC processes [Osicka 2022]. In case of tools with a larger cutting edge radius, the contact area increases, thereby elevating the friction between the tool and the machined material. This phenomenon is even more pronounced when machining materials with poor thermal conductivity, where a larger portion of the heat must be dissipated by alternative means. The use of cooling can have a negative impact not only on tool life but also on workpiece

quality. An inappropriate choice of cutting environment can induce residual tensile stresses within the surface layer due to thermal imbalance [Liu 2022]. The objective of modern machining is to eliminate tensile stresses in the material, as their occurrence is associated with adverse effects on workpiece quality, such as microcracks, fatigue, and corrosion [Kuhlmann 2024]. To achieve such surface integrity while fulfilling contemporary ecological standards, process parameters must be optimized with respect to both tool microgeometry and dynamic stability. In this context, Vozar et al. [2025] statistically evaluated how four cutting-edge radii influence tangential and radial cutting forces during the milling of AISI 316L stainless steel. Quantifying this force increase provides vital data for energy-efficient machining, aligning process optimization with Green Deal mandates for carbon footprint reduction in manufacturing. Furthermore, these cutting forces are inherently linked to the excitation of system instability. Addressing this issue, Olejarova and Krenicky [2022] utilized FFT spectrum analysis to investigate vibration amplitudes during milling at spindle speeds between 1200 and 1600 rpm. Minimizing these vibrations not only prevents surface degradation but directly contributes to sustainable machining and Green Deal goals by reducing overall energy consumption and preventing premature scrap production. The study focuses on an experimental analysis of the effect of various cutting environments on tool life in high-feed milling technology. In addition to evaluating tool wear, the research is expanded to assess the energy consumption of the process and calculate the carbon footprint (CF_{1h}) of individual cutting environment variants. While historical studies demonstrated that the dominant failure mechanism of milling tools is thermal cracking caused by cyclic loading [Peters 1992], contemporary research in HFM must extend these findings to include modern aspects related to the sustainability of the entire process, including energy balance and carbon footprint. The main objective of the study is therefore to identify the optimal cutting environment that, under the given cutting conditions, represents the best synergy between tool life, energy efficiency, and environmental sustainability of the analyzed machining process.

2 EXPERIMENTAL SETUP AND METHODOLOGY

To ensure the reproducibility of the results and the accuracy of the analysis, the experiments were carried out under pre-defined, constant conditions (see experimental setup in Fig. 1). For the HFM experiments, a tool assembly consisting of a cutter body and indexable inserts from the manufacturer Dormer Pramet was selected. A milling cutter with a diameter of D = 50 mm, equipped with internal channels for supplying the process fluid or compressed air directly into the cutting zone, was chosen (tool catalog designation: 50A07R-SM OSO09-C-P1). According to the manufacturer, the design of the cutter body is optimized to minimize vibrations at high feed rates. Square-shaped indexable inserts with a special geometry designed for HFM applications were used for the experiment (catalog designation: SOHT 090414SR-M-P1). This geometry utilizes a small setting angle Kr, which enables chip thickness transformation and allows extreme feed rates to be achieved at small axial depths of cut (ap). The insert material is equipped with a multi-layer AlTiN-based PVD coating, providing the tool with enhanced resistance against abrasive wear and thermal loading. The values of the applied cutting conditions are presented in Tab. 1.

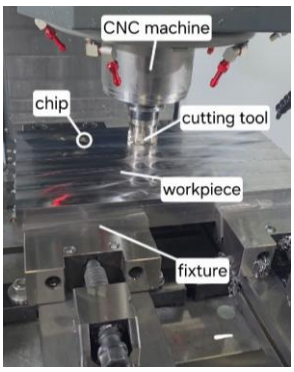


Figure 1. Experimental setup.

Table 1. Cutting conditions utilized for the experimental testing.

v_c [m.min^{-1}]	n [min^{-1}]	a_p [mm]	a_e [mm]	f_z [mm]	v_f [mm.min^{-1}]
270	2305	0.5	37	0.56	1290.8

The X37CrMoV5-1 tool steel (according to EN ISO 4957, corresponding to AISI H11) was selected for the experimental machining. The chemical composition of the material is presented in Tab. 2 [Lucefin 2018]. The steel is alloyed with chromium, molybdenum, and vanadium. According to the material datasheets, its typical properties include good strength, toughness, and resistance to thermal shocks [Lucefin 2018, Base-Do Steel 2026]. The material was in a quenched and tempered state with a hardness of 300 HB, which represents a standard industrial value for roughing and semi-finishing operations of molds and dies [Base-Do Steel 2026].

Table 2. Chemical composition of X37CrMoV5-1 steel [wt. %].

C	Si	Mn	P	S	Cr	Mo	V
0.33-0.41	0.80-1.20	0.25-0.50	Max 0.03	max 0.02	4.80-5.50	1.10-1.50	0.30-0.50

Due to the material intensity and long cutting durations of the HFM tests, a standardized single-edge degradation tracking procedure was applied for each cutting. To ensure measurement repeatability of flank wear (VB_B), the indexable insert was clamped in the same place throughout the test, and measurements were recorded in a rigid positioning fixture under controlled optical alignment. The tool life criterion was defined as VB_B = 0.3 mm in accordance with the ISO 8688-2 standard [ČSN ISO 8688-2 1993]. Tool wear evaluation and microscopic analysis were performed using an Olympus SZX10 stereo microscope. To ensure strict measurement repeatability and consistent image acquisition, the indexable inserts were fixed in a custom rigid positioning fixture.

To analyze energy efficiency and determine the environmental impact (carbon footprint, CF_{1h} [kg CO2eq]), the electrical power consumption of the machining center was monitored continuously. A Hioki PW3360 three-phase power analyzer and logger was connected directly to the main power supply line of the machining center via three-phase current probes. Active power data P(t) [W] were logged at a sampling interval of 1 s. Before starting each machining test, a baseline calibration was performed by recording the machine's idle power consumption (P_{idle} = 1000 W) over a 5-minute period under stable operating conditions (spindle running at test speed without cutting engagement). The net cutting power was subsequently evaluated by subtracting the idle power consumption (P_{idle}) of the machine tool from the active power consumption recorded during full engagement cutting passes.

3 ANALYSIS OF TOOL WEAR AND POWER CONSUMPTION

The first key indicator of the cutting environment's efficiency was the evolution of tool flank wear (VB_B) as a function of cutting time (t), as shown in Fig. 2. The measured data reveal

a fundamental difference in tool behavior when using a process fluid compared to strategies utilizing gaseous media or dry machining. For the methods employing conventional external liquid cooling (1.5 bar) and high-pressure internal liquid cooling (21 bar), a very short phase of stable wear can be observed (critical wear-over-time progressions for Sample B and Sample C). A significant turning point in the graph occurs after approximately 15 minutes of net cutting time. Sample B exhibits a steep, almost exponential increase in the wear value, which exceeded the specified criterion (VB_B = 0.3 mm) before the 25th minute. Sample C (internal liquid cooling through the tool) exhibited a slightly more linear progression compared to external liquid cooling; however, after 20 minutes in the cut, rapid degradation of the cutting edge followed, leading to total failure after 26 minutes. This phenomenon can be attributed to the high intensity of thermal shocks. In high-feed milling, the cutting edge undergoes cyclic heating within the cutting zone, followed by rapid cooling by the process fluid stream as the tool exits the cut. This elevated thermal stress can lead to the initiation of thermal cracks and subsequent chipping of the functional part of the cutting tool edge.

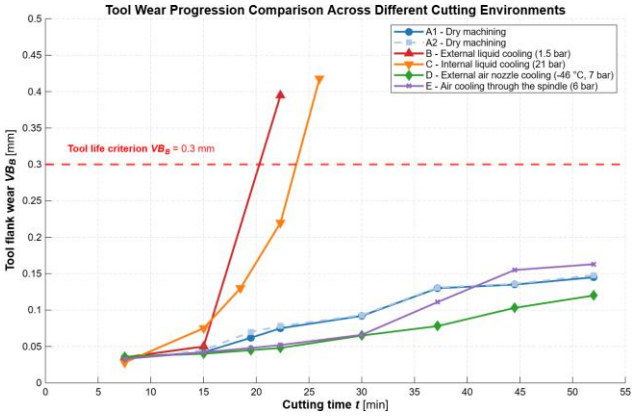


Figure 2. Evolution of tool wear for the tested tools in various cutting environments.

A completely opposite trend is exhibited by the dry machining strategies. All of these variants achieved cutting times exceeding 50 minutes without reaching the tool life criterion of VB_B = 0.3 mm. Sample A1 and Sample A2 (dry machining) demonstrated consistency and stability with a gradual increase in tool flank wear. The thermal resistance of the selected cutting tool was not exceeded, as the cutting environment did not act as a catalyst for thermal shocks. The wear progression of Sample D (external air nozzle with sub-zero compressed air at -46 °C) appears to be the most effective in terms of tool life. This wear curve exhibits the shallowest slope (the lowest wear rate), suggesting that the low air temperature can effectively lower the temperature within the cutting zone while simultaneously assisting in chip evacuation without adversely affecting the integrity of the PVD coating and the carbide structure of the cutting tool. Sample E (compressed air cooling through the spindle) achieved comparable results to dry machining, with a slight increase in wear during the final phase of the test (after the 40th minute). As evident from the graph in Fig. 2, the application of a cutting fluid in HFM machining of X37CrMoV5-1 steel under the given cutting parameters leads to a reduction in tool life of more than 60% compared to energy-efficient and environmentally friendly methods.

Visual analysis of the tool flank after the completion of the tests confirms the assumptions derived from the wear kinetics. Figure 3 illustrates the condition of the cutting edges for all five tested environments. For Sample A1, Sample A2 (dry machining), Sample D (compressed air), and Sample E (air through the spindle), the test was stopped after 52 minutes of net cutting time. Although these tools did not reach the critical value of VB_B = 0.3 mm, the test was terminated because high process stability had been demonstrated and to conserve workpiece material. Images (a), (b), (e), and (f) reveal a highly uniform and gradual flank wear without any signs of chipping. In stark contrast, Sample B (external liquid cooling) and Sample C (internal liquid cooling through the tool) exhibit total degradation of the cutting edge in images (c) and (d). Severe chipping of the functional part of the cutting edge and the formation of deep craters are clearly visible. This failure occurred after just 22.3 minutes of machining for Sample B and after 26 minutes for Sample C. The absence of steady wear and the presence of chipped cutting edge sections confirm that the dominant degradation mechanism in the liquid environment is not abrasion, but rather a brittle fracture initiated by thermal fatigue.

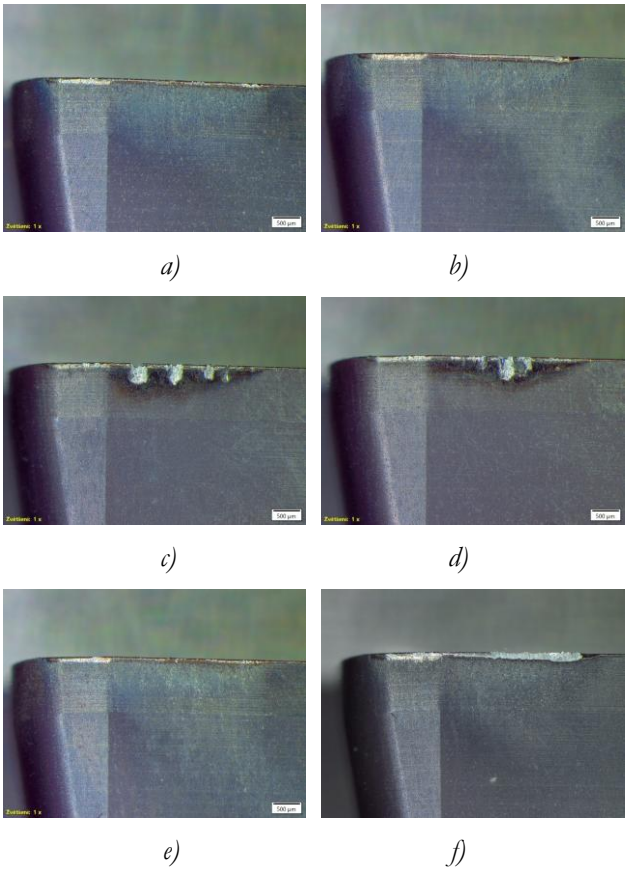


Figure 3. Tool wear after experimental testing – sample (a) A1 (t = 52 min); (b) sample A2 (t = 52 min); (c) sample B (t = 22,3 min); (d) sample C (t = 26 min) (e) sample D (t = 52 min); (f) sample E (t = 52 min).

To clarify the failure progression under liquid environment, the sequential damage of Sample C (high-pressure internal liquid cooling) was monitored via optical microscopy (Fig. 4). Microscopic observations reveal the physical damage sequence. In the initial phases (t = 7.5 to 15 min), the tool exhibits relatively stable behavior with a minor increase in the wear land. However, even at this stage, microscopic thermal cracks perpendicular to the cutting edge are initiated due to the cyclic temperature fluctuations (see Fig. 4b). Between the 18th and 22nd minute, these cracks began to coalesce, weakening the structure of the carbide substrate itself. Image (d) already illustrates the onset of micro-chipping of small

material particles from the functional part of the cutting tool edge. The final image (e) demonstrates how, in the ultimate stage, individual thermal cracks merge, leading to the catastrophic chipping of a larger section of the cutting edge material. At this point, the tool completely loses its functional geometry, resulting in a sharp increase in cutting forces and vibrations, rendering the tool further unusable. This sequential view in Fig. 4 clearly proves that the application of a cutting fluid in HFM machining of X37CrMoV5-1 steel under the given cutting conditions is counterproductive. This observed damage mechanism is physically driven by thermal shock fatigue. While liquid cooling may be beneficial in conventional milling, at high cutting speeds and feed rates, it induces a temperature gradient that is destructive to the carbide tool.

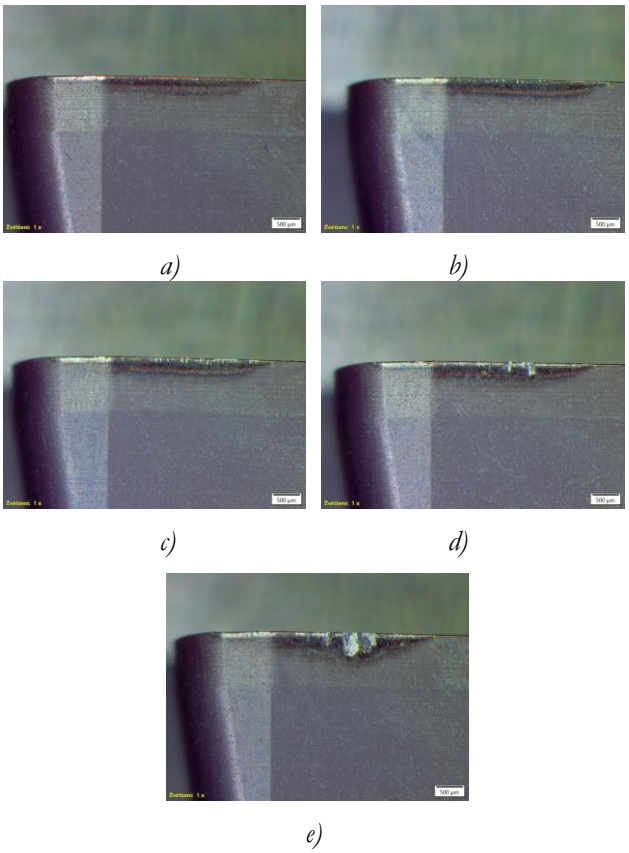


Figure 4. Tool wear after experimental testing – sample C (internal cooling) – (a) after 7,5 min (b) after 15 min (c) after 18,75 min (d) after 22,5 min (e) after 26,25 min.

In addition to tool life, energy consumption is a key factor in modern manufacturing engineering. Figure 5 illustrates an exemplary time-progression recording of the machine's instantaneous active power consumption P(t) [W] during machining in an environment with internal liquid cooling (Sample C). The recording clearly identifies six cycles (passes) of active material removal. The peaks reaching values of approximately 3,350 W represent the full engagement phase of the cut (rated cutting power), while the drop to values around 1,000 W at the end of the graph corresponds to the idle power consumption (P_{idle}) of the machine tool.

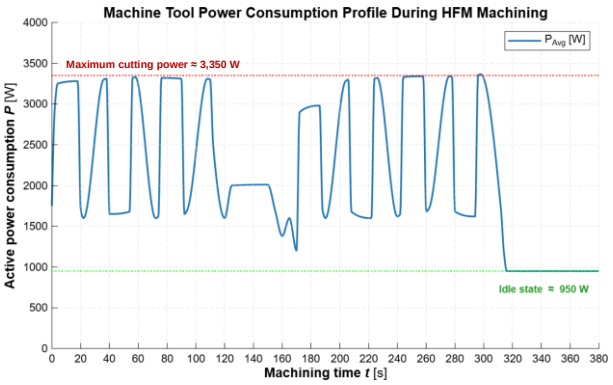


Figure 5. Machine power consumption analysis during HFM machining – sample C.

For an objective comparison of all variants, the specific cutting energy e_{cut}, expressed in J·mm^{-3}, was determined [Zhao 2017]. This parameter indicates the amount of energy required to remove a unit volume of material and is defined by the following relation:

$$e_{cut} = (P_{total} - P_{idle}) / MRR, \quad (1)$$

where P_{idle} is the idle power consumption of the spindle and axes, P_{total} is the total measured power input and MRR is the material removal rate, which for the given cutting conditions amounts to 23,879.8 mm^3·min^{-1} (see Eq. 2 and 3).

Calculation of material removal rate:

$$MRR = a_p \cdot a_e \cdot v_f \quad (2)$$

$$MRR = a_p \cdot a_e \cdot f_z \cdot z \cdot n = 0.5 \cdot 37 \cdot 0.56 \cdot 1 \cdot 2305 \quad (3)$$

$$MRR = 23{,}879.8\ mm^3 \cdot min^{-1} = 23.88\ cm^3 \cdot min^{-1},$$

where: a_p – axial depth of cut [mm],
a_e – radial depth of cut [mm],
v_f – feed rate [mm·min^{-1}],
f_z – feed per tooth [mm],
z – number of teeth [-],
n – spindle speed [min^{-1}].

Based on the measured average power inputs (P_{avg}), the specific cutting energy e_{cut} and the carbon footprint per 1 hour of machining CF_{1h} [kgCO_2eq], representing the hourly emissions produced during machining within the given cutting environment, were calculated. The results are presented in Tab. 3. To calculate the net cutting power, the idle power consumption of the machine tool (P_{idle} = 1,000 W), determined from the analysis of process intervals, was subtracted from the total average power input.

Table 3. Comparison of energy and environmental parameters for different cutting environments.

Cutting environment	Average power P_{avg} [W]	Specific cutting energy e_{cut} [J . mm^3]	Carbon footprint (1 h) [kg CO_2]
Sample A - dry machining	2400	3.52	1.04
Sample B - external liquid cooling (1.5 bar)	3400	6.03	1.48
Sample C - internal liquid cooling (21 bar)	3350	5.90	1.45
Sample D external air noozle cooling (-46°C, 7 bar)	2650	4.15	1.15
Sample E compressed air cooling (6 bar)	2450	3.64	1.06

4 DISCUSSION

The following key findings can be derived from the results presented in Tab. 3 and the preceding wear analyses:

Liquid cooling methods (Sample B and Sample C) exhibit nearly twice the specific cutting energy (e_{cut}) compared to dry machining. This increase is primarily driven by the high power consumption of the pumps and hydraulic losses within the system. Combined with the lower tool life, liquid cooling appears completely unsuitable for HFM machining of X37CrMoV5-1 steel under the given cutting conditions and with the selected tooling.

Sample A (dry machining) is the most energy-efficient regarding machine tool power consumption. Sample A achieved the lowest carbon footprint during machining (1.04 $kg.h^{-1}$). Given the long tool life and the absence of costs associated with process media, this represents a highly sustainable method.

Sample D and Sample E (compressed air cooling) exhibit a slightly higher power input than dry machining (an increase of 50–250 W on the machine tool side). Although the data do not include compressor power consumption, from a technological standpoint (particularly for variant D with sub-zero compressed air), these methods offer the highest process stability and the lowest cutting edge wear.

It must be emphasized that the actual environmental impact of the variants utilizing compressed air (Sample D and Sample E) would likely be the highest if compressor efficiency were taken into account in the overall life-cycle inventory. However, from the perspective of workplace cleanliness and the elimination of hazardous waste disposal (issues related to process fluid management), these dry machining variants represent an environmentally more favorable alternative than conventional cooling with process fluids.

5 RESULTS

The presented study investigated the influence of five different cutting environments on the high-feed milling process of X37CrMoV5-1 tool steel. Based on the experimental data, cutting edge wear analysis, and energy consumption measurements, the following conclusions can be formulated:

- The application of conventional cutting fluids was found to promote premature tool failure under the tested high-feed milling conditions. Within the evaluated 52-minute time window, liquid cooling reduced the effective operational cutting time by more than 50–60% compared to dry machining. The primary failure mechanism was thermal shock, which initiated the formation of comb cracks and subsequent chipping of the cutting tool edge material. Their occurrence is caused by the significantly different thermophysical properties of the applied process media, particularly their specific heat capacity. Given that the specific heat capacity of the cutting fluid exceeds that of air approximately fourfold, its application results in a much more aggressive heat dissipation from the cutting edge surface. Under interrupted cutting conditions, the fluid generates intense thermal shocks and high temperature gradients, which are the primary cause of the initiation and propagation of comb cracks. Paradoxically, the lower cooling intensity of air manifests as higher thermal stability of the cutting edge, similar to dry machining.
- Strategies utilizing compressed air cooling and dry machining demonstrated high stability of the cutting process. The tools exhibited gradual and predictable wear (flank wear VB_B on the major cutting edge). After 52 minutes of net cutting time, these samples did not reach the critical wear criterion (VB_B = 0.3 mm).
- Dry machining exhibited the lowest machine power consumption and the lowest carbon footprint 1.04 kg $CO_2 \cdot h^{-1}$). Fluid-based methods are the most energy-intensive due to pump operation, which increases the overall cost of the machining process execution.

An interesting finding is the difference in average power consumption between dry machining (2400 W) and compressed air cooling (2450–2650 W), even though the energy consumption of the compressor was not included in the measurements. This phenomenon can be explained by two factors:

- Effective air cooling reduces the temperature in the cutting zone. The lower temperature of the steel at the deformation zone increases its resistance to deformation (higher yield strength at elevated temperatures), leading to an increase in cutting forces and a consequently higher spindle load during the cutting process execution.
- In dry machining, higher heating occurs, which can act to a certain extent as a "plasticizer" (thermal softening effect) within the shear zone. Paradoxically, this decreases the required spindle torque compared to the intensively cooled processes of the other variants.

For HFM operations, the elimination of cutting fluids is generally recommended. While compressed air cooling effectively balances tool life and process stability, the high energy demand of air compression impairs its overall environmental efficiency. Consequently, dry machining represents the most sustainable and economically viable alternative among the investigated options, offering minimal energy consumption.

ACKNOWLEDGMENTS

This research study was supported by the grant "Comprehensive technology for interdisciplinary work with advanced materials, emphasizing their multidisciplinary applications.", FSI-S-25-8787.

REFERENCES

Paper in a journal:

[Jacquet 2025] Jacquet, T., Guyon, J.-B., Viprey, F., Fromentin, G. and Prat, D. Contribution to the analytical determination of uncut chip thickness for cutting force modelling in milling with refinements for high-feed milling. CIRP Journal of Manufacturing Science and Technology, 2025, Vol. 63, pp 240-264.

[Huang 2021] Huang, F. and Jin, X. Surface texture generation using high-feed milling with spindle speed modulation. Precision Engineering, 2021, Vol. 72, pp 13-24.

[Olejarova 2022] Olejarova, S. and Krenicky, T. Development of vibrations due to changing spindle speeds during

milling. Online. *MM Science Journal*. 2022, roč. 2022, č. 3, s. 5949-5953. ISSN 1803-1269.

[Osicka 2022] Osicka, K., Zouhar, J., Sliwkova, P. and Chladil, J. Cutting Force When Machining Hardened Steel and the Surface Roughness Achieved. Applied Sciences-Basel, 2022, Vol. 12, No. 22, 21 p.

[Peters 1992] Peters, J.E. and Hoefler, B. Relationship between carbon chemistry and thermal cracking resistance in carbide milling inserts. International Journal of Refractory Metals and Hard Materials, 1992, Vol. 11, No. 3, pp 159-163.

[Vozar 2025] Vozar, M., Vopat, T., Jurina, F., Patoprsty, B. Statistical evaluation of cutting force components as a function of cutting edge radius size for milling of austenitic stainless steel AISI 316L. Online. *MM Science Journal*. 2025, roč. 2025, č. 1. ISSN 1803-1269.

[Zhao 2017] Zhao, G.Y., Liu, Z.Y., He, Y., Cao, H.J. and Guo, Y.B. Energy consumption in machining: Classification, prediction, and reduction strategy. Energy, 2017, Vol. 133, pp 142-157.

Paper in proceedings:

[Kuhlmann 2024] Kuhlmann, G., Borysenko, D., Solter, J. and Karpuschewski, B. Simultaneous high-speed cutting and high-feed milling: An investigation on surface integrity. Procedia CIRP, 2024, Vol. 123, pp 59-64.

[Gyliene 2016] Gyliene, V. and Eidukynas, V. The numerical analysis of cutting forces in High Feed face milling, assuming the milling tool geometry. Procedia CIRP, 2016, Vol. 46, pp 436-439.

[Bleicher 2018] Bleicher, F. and Reiter, M. Wear reduction on cutting inserts by additional internal cooling of the cutting edge. Procedia Manufacturing, 2018, Vol. 21, pp 518-524.

[Liu 2022] Liu, H., Schraknepper, D. and Bergs, T. Investigation of residual stresses and workpiece distortion during high-feed milling of slender stainless steel components. Procedia CIRP, 2022, Vol. 108, pp 495-500.

[Majerik 2015] Majerik, J. and Jambor, J. Computer Aided Design and Manufacturing Evaluation of Milling Cutter when High Speed Machining of Hardened Steels. Procedia Engineering, 2015, Vol. 100, pp 450-459.

WWW page:

[Dormer Pramet 2024] DORMER PRAMET. Milling Indexable 2024: EN [online]. 2024 [cited 2026-01-13]. Available from: https://5wyuco84ao39w9tsgkkmnmx.blob.core.windows.net/cms/MILLING-INDEXABLE-2024-EN.pdf

[Lucefin Group 2018] LUCEFIN GROUP. 1.2343 X37CrMoV5-1: Technical card [online]. 2018 [cited 2026-01-13]. Available from: https://www.lucefin.com/oaleekso/files_mf/15236074671.2343X37CrMoV51.pdf

[Base-Do Steel 2026] BASE-DO STEEL. Material 1.2343 [online]. 2026 [cited 2026-01-13]. Available from: https://www.basedosteel.com/en/materials/material/Materials/12343.html

Technical Standards:

[ČSN ISO 8688-2 1993] ČSN ISO 8688-2. Zkoušky životnosti frézovacích nástrojů - Část 2: Čelní frézování. Praha: Federální úřad pro normalizaci a měření, 1993. Třídicí znak 220450.

CONTACTS:

Ing. Martin Drbal
Brno University of Technology, Faculty of Mechanical Engineering, Technicka 2 Brno, Czech Republic
541 142 406; e-mail: martin.drbal@vutbr.cz

LICENSE CREATIVE COMMONS:

The article is published under the terms and conditions of the Creative Commons Attribution 4.0 International License (CC BY 4.0).